Supporting Information

Disorder Induced Polymorphic Transitions in the High Hydrogen Density Compound $Sr(BH_4)_2(NH_3BH_3)_2$

Mathias Jørgensen,[1] Young-Su Lee,[2] Morten Bjerring,[1] Lars H. Jepsen,[3] Ümit Akbey,[1] Young Whan Cho,[2] Torben R. Jensen[1]*

[1]*Interdisciplinary Nanoscience Center (iNANO) and Department of Chemistry, University of Aarhus, DK-8000 Aarhus, Denmark*

[2]*High Temperature Energy Materials Research Center, Korea Institute of Science and Technology, Seoul 02792, Republic of Korea*

[3]*Danish Technological Institute, Aarhus, Denmark*

*Corresponding Author Torben R. Jensen, trj@chem.au.dk

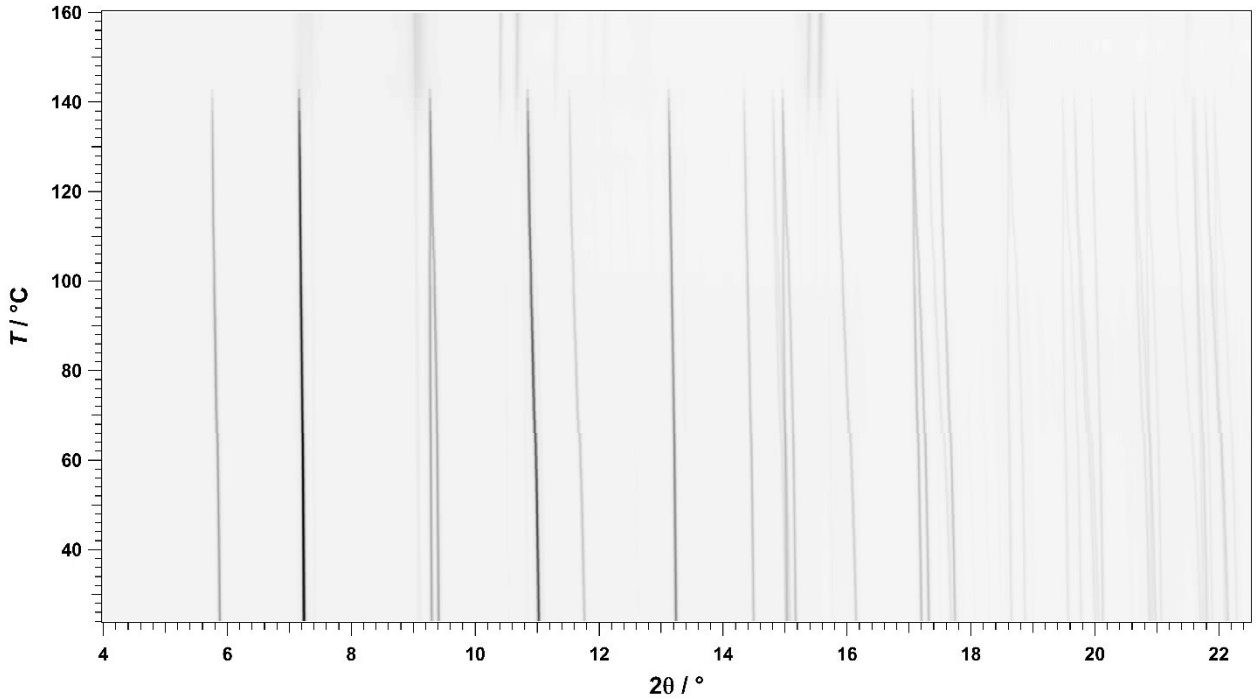

Figure S1: *In situ* SR-PXD data of $Sr(BH_4)_2(NH_3BH_3)_2$ measured at the Swiss-Norwegian beamline (BM02.1) at ESRF, Grenoble, France from *RT* to 160 °C at a heating rate of 5 °C/min. λ = 0.69449 Å.

Table S1: Atomic positions and thermal displacement parameters for the structural model of *α*-$Sr(BH_4)_2(NH_3BH_3)_2$. The SR-PXD data (measured at *RT*) and Rietveld refinement profile is shown in figure S2.

	Wyckoff site	x	y	z	U (Å^2)
B1	8c	0.7364(12)	0.4895(8)	0.2385(17)	0.020(3)
H1	8c	0.6736(12)	0.5661(8)	0.2766(17)	0.02533
H2	8c	0.6694(12)	0.4201(8)	0.2943(17)	0.02533
H3	8c	0.8754(12)	0.4906(8)	0.2757(17)	0.02533
H4	8c	0.7264(12)	0.4829(8)	0.0951(17)	0.02533
Sr	4b	0.5	0.5	0.5	0.0174(4)
B2	8c	0.9621(14)	0.2827(4)	-0.0510(9)	0.029(5)
H5	8c	0.8799(14)	0.2592(4)	-0.1554(9)	0.02533
H6	8c	0.8932(14)	0.3266(4)	0.0461(9)	0.02533
H7	8c	1.0761(14)	0.3247(4)	-0.0934(9)	0.02533
N	8c	1.0211(12)	0.1832(2)	0.0279(10)	0.071(3)
H8	8c	1.0933(12)	0.1969(2)	0.1198(10)	0.02533
H9	8c	0.9296(12)	0.1422(2)	0.0680(10)	0.02533
H10	8c	1.0822(12)	0.1406(2)	-0.0485(10)	0.02533

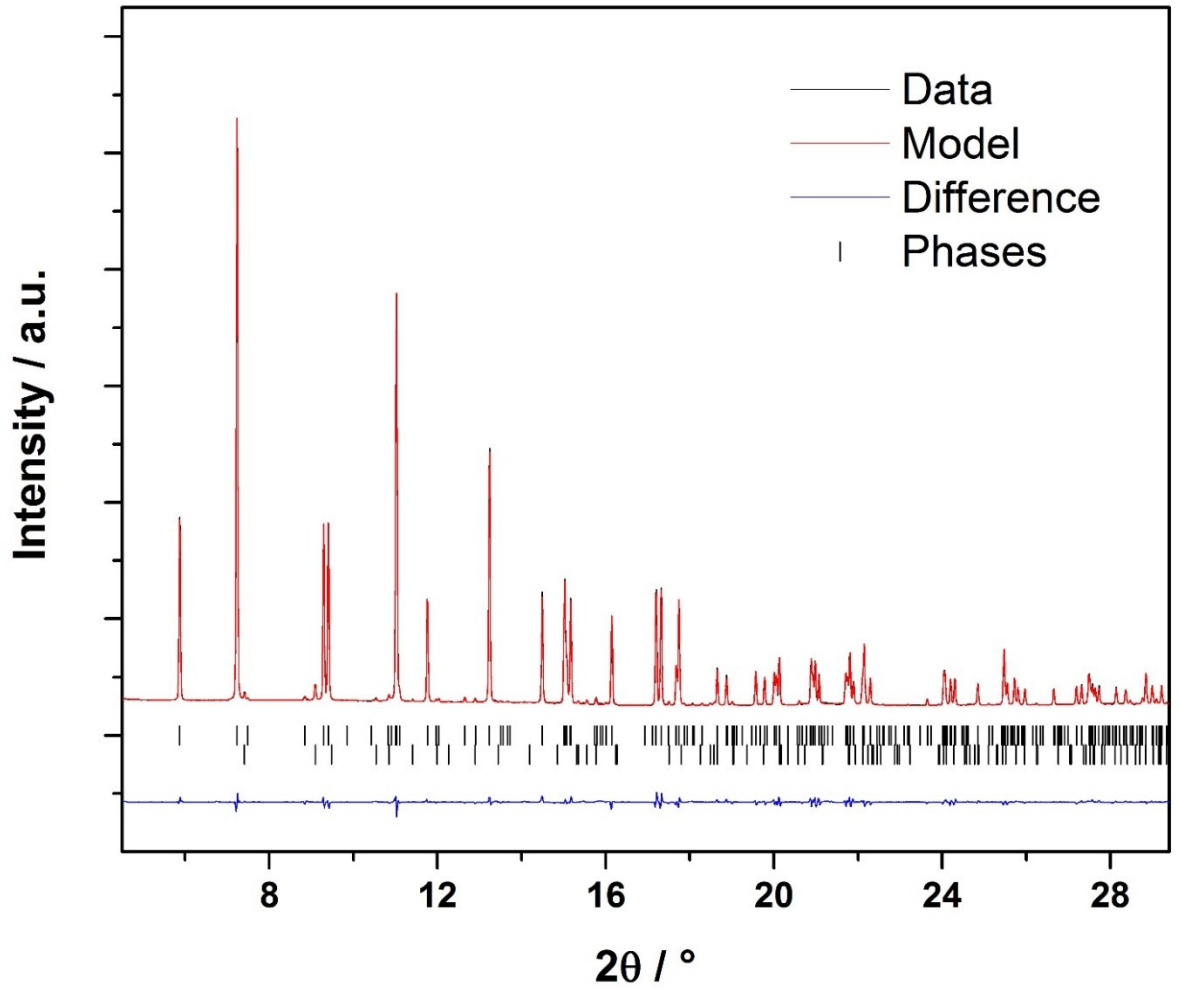

Figure S2: Model fit to data for α-$Sr(BH_4)_2(NH_3BH_3)_2$ with space group *Pbca* and unit cell parameters a = 8.47448(5), b = 13.56266(9) and c = 8.57407(6) Å. The SR-PXD data was measured at the Swiss-Norwegian beamline (BM02.1) at ESRF, Grenoble, France at *RT*. λ = 0.69449 Å. χ^2 = 477, R_{Bragg} = 2.21 %. Upper ticks: α-$Sr(BH_4)_2(NH_3BH_3)_2$, lower ticks: $Sr(BH_4)_2$.

Table S2: Atomic positions and thermal displacement parameters for the structural model of β-$Sr(BH_4)_2(NH_3BH_3)_2$. The SR-PXD data (measured at T = 70 °C) and Rietveld refinement profile is shown in figure S3.

	Wyckoff site	x	y	z	U (Å^2)
B1	8b	0.7166(17)	0.0162(12)	0.7246(15)	0.012(6)
H1	8b	0.6690(17)	0.0918(12)	0.7860(15)	0.038
H2	8b	0.7194(17)	-0.0486(12)	0.8243(15)	0.038
H3	8b	0.6323(17)	-0.0110(12)	0.6164(15)	0.038
H4	8b	0.8470(17)	0.0322(12)	0.6700(15)	0.038
Sr	4a	0	0	0.5	0.0344(6)
B2	8b	0.5562(11)	0.2843(3)	-0.5263(16)	0.039(6)
H5	8b	0.6772(11)	0.2700(3)	-0.5991(16)	0.038
H6	8b	0.4576(11)	0.3246(3)	-0.6079(16)	0.038
H7	8b	0.5842(11)	0.3319(3)	-0.4087(16)	0.038

N	8b	0.4887(11)	0.1810(3)	-0.4740(16)	0.070(3)
H8	8b	0.5570(11)	0.1490(3)	-0.3891(16)	0.038
H9	8b	0.4813(11)	0.1327(3)	-0.5669(16)	0.038
H10	8b	0.3797(11)	0.1869(3)	-0.4250(16)	0.038

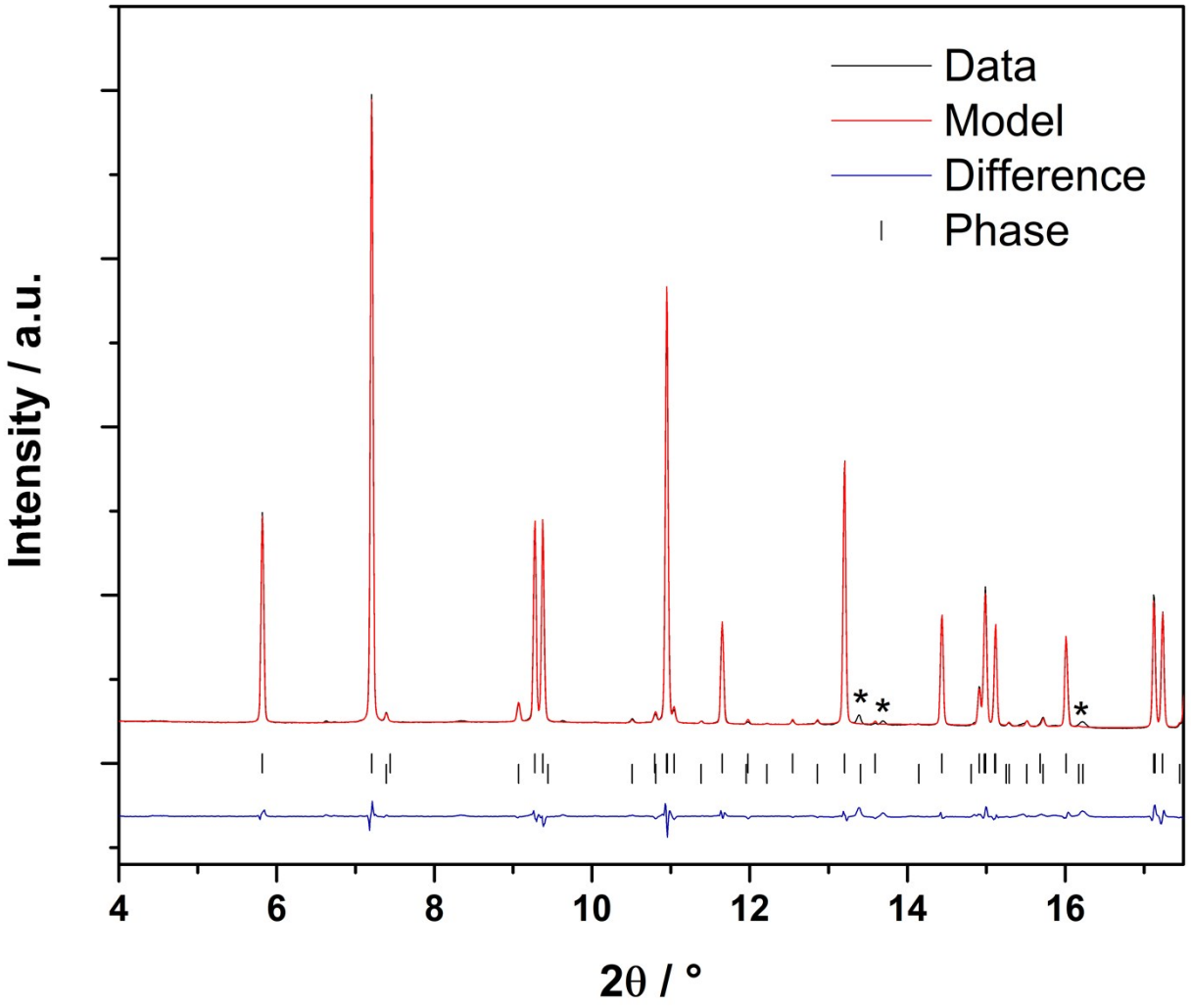

Figure S3: Model fit to data for β-$Sr(BH_4)_2(NH_3BH_3)_2$ with space group *Aba*2 and unit cell parameters a = 8.5930(1), b = 13.6887(2) and c = 8.5007(1) Å. The SR-PXD data was measured at the Swiss-Norwegian beamline (BM02.1) at ESRF, Grenoble, France at T = 70°C. λ = 0.69449 Å. χ^2 = 941, R_{Bragg} = 3.58 %. Upper ticks: β'-$Sr(BH_4)_2(NH_3BH_3)_2$, lower ticks: $Sr(BH_4)_2$. Asterisks identify the three most intense peaks of the super structure.

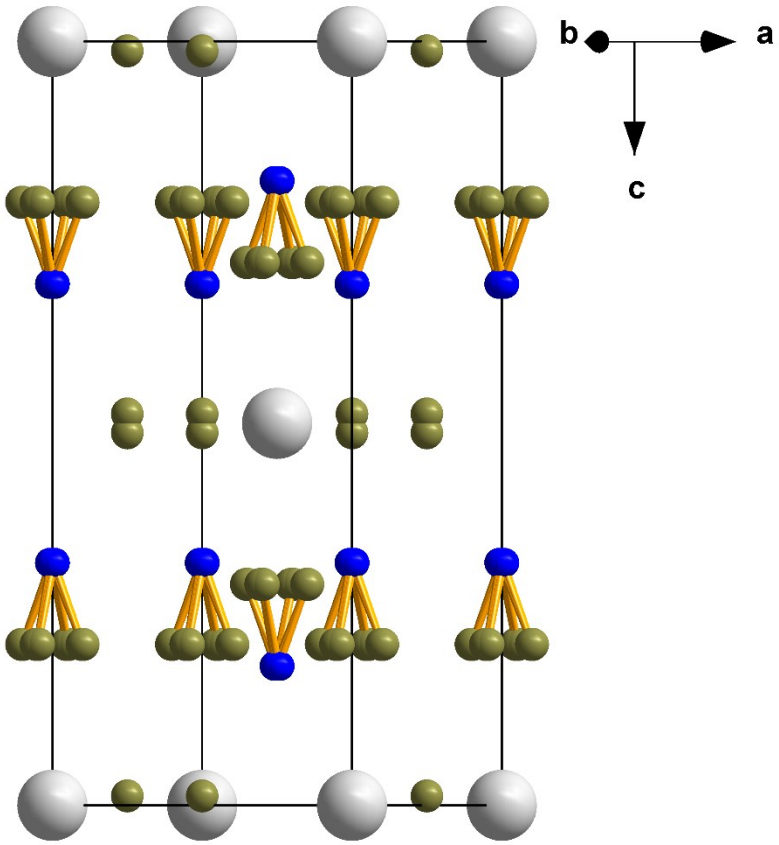

Figure S4: Disordered high temperature model of $Sr(BH_4)_2(NH_3BH_3)_2$ with space group *I*4/*mmm* and unit cell parameters a = 6.07589(5) and c = 13.83468(12) Å. The model suggests a more free coordination of the BH_3 moiety of the ammonia borane molecule to Sr, while the NH_3 moiety is less mobile. Yellow: B, Blue: N, Gray: Sr. Hydrogen atoms have been omitted for clarity.

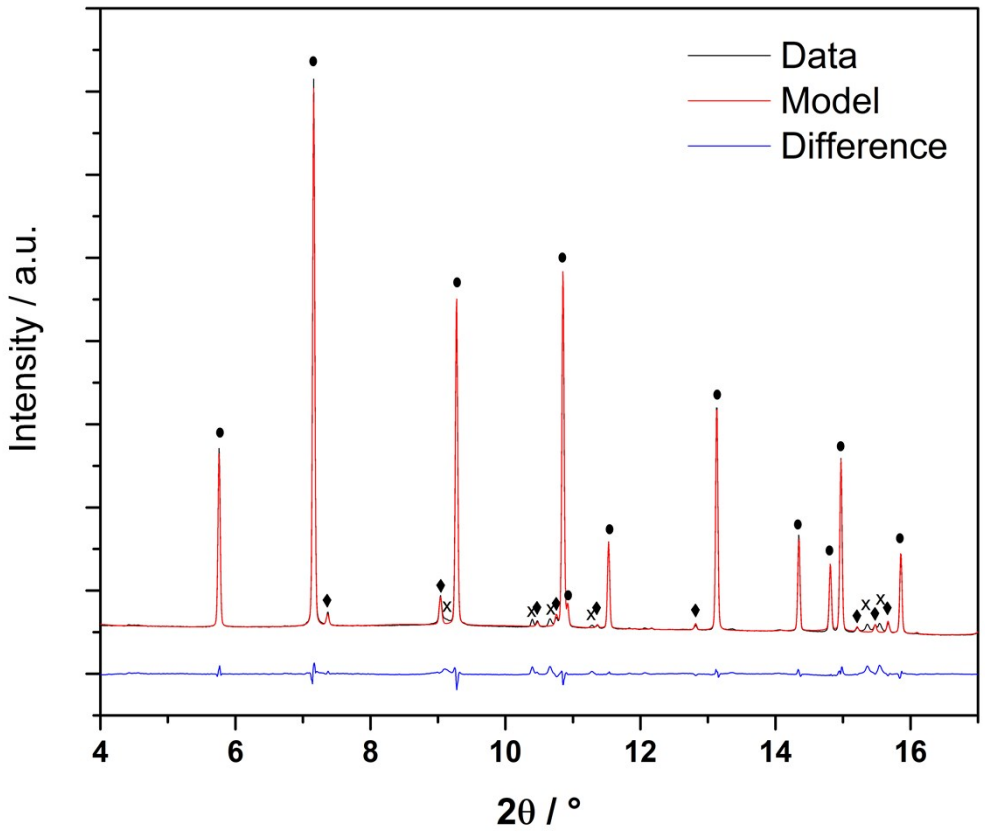

Figure S5: Model fit to HT data of $Sr(BH_4)_2(NH_3BH_3)_2$ based on the disordered model (*I*4/*mmm*). Circles: $Sr(BH_4)_2(NH_3BH_3)_2$, diamonds: $Sr(BH_4)_2$, cross: disordered $Sr(BH_4)_2$. Notice the broadening of the first visible peak of the disordered $Sr(BH_4)_2$.

In order to characterize the sample we applied solid-state NMR spectroscopy. In Fig. S6 a ^{1}H NMR spectrum of $Sr(BH_4)_2(NH_3BH_3)_2$ acquired under fast MAS conditions is shown.

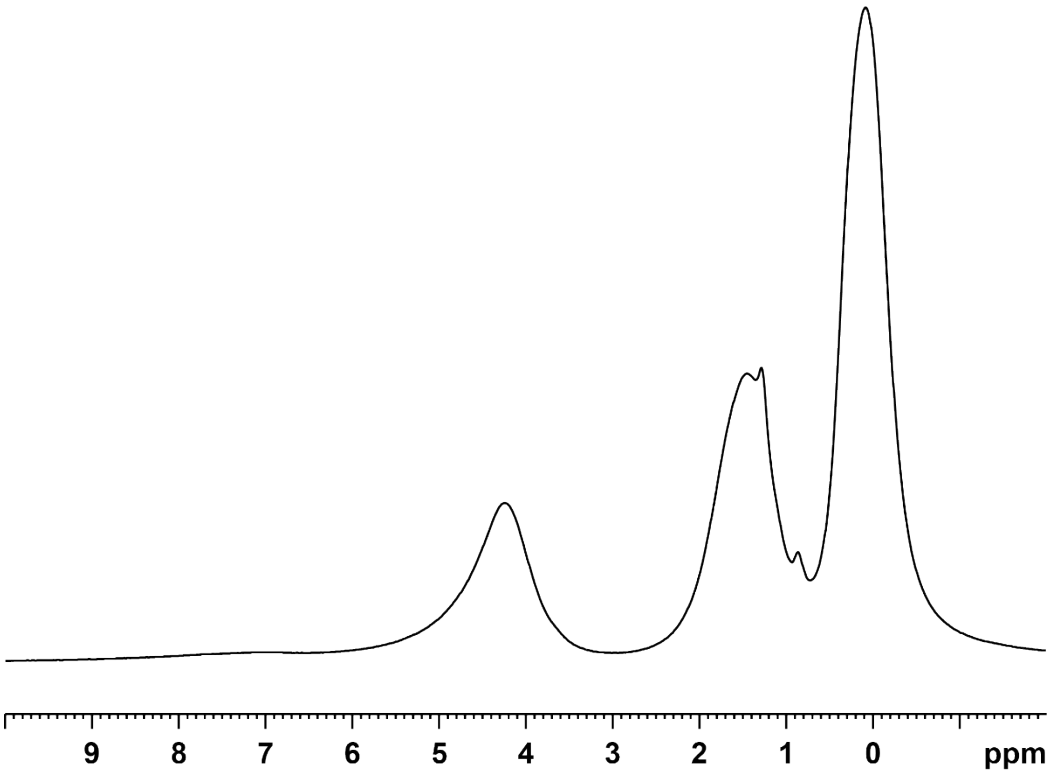

Figure S6: ^{1}H MAS NMR (700 MHz, ν_R = 60 kHz) of $Sr(BH_4)_2(NH_3BH_3)_2$ showing three distinct peaks at 0.1 ppm, 1.5 ppm, and 4.2 ppm assigned to BH_4^-, BH_3, and NH_3, respectively.

As expected, the spectrum shows three major peaks around 0.1 ppm, 1.5 ppm, and 4.2 ppm. In addition, two small peaks are seen around 0.9 ppm and 1.3 ppm. In a double-quantum filtered spectrum at otherwise identical conditions, these additional peaks vanish as seen in Fig. 5 (main text), and they are therefore not part of the rigid structure. Hence we ascribe these peaks as impurities in the sample.

To help assigning the three peaks an isotopically enriched sample of $^{15}NH_3BH_3$ was synthesized. 1D ^{1}H (a), 1D double-quantum filtered ^{1}H (b), 1D ^{15}N (c), and 2D HETCOR ^{1}H-^{15}N spectra (d) of this sample are shown in Fig. S7. The ^{1}H spectrum acquired at 60 kHz MAS shows two signals at approx. 1.3 ppm and 4.2 ppm while the ^{15}N spectrum gives a single signal at 16.0 ppm. In the 2D spectrum the ^{15}N spin is correlated to the protons at 4.2 ppm, which are therefore assigned to the NH_3 group. The ^{1}H signal at 1.3 ppm is then assigned to BH_3, and in the $Sr(BH_4)_2(NH_3BH_3)_2$

sample the signals at 0.1 ppm, 1.5 ppm, and 4.2 ppm are assigned to BH_4, BH_3, and NH_3, respectively.

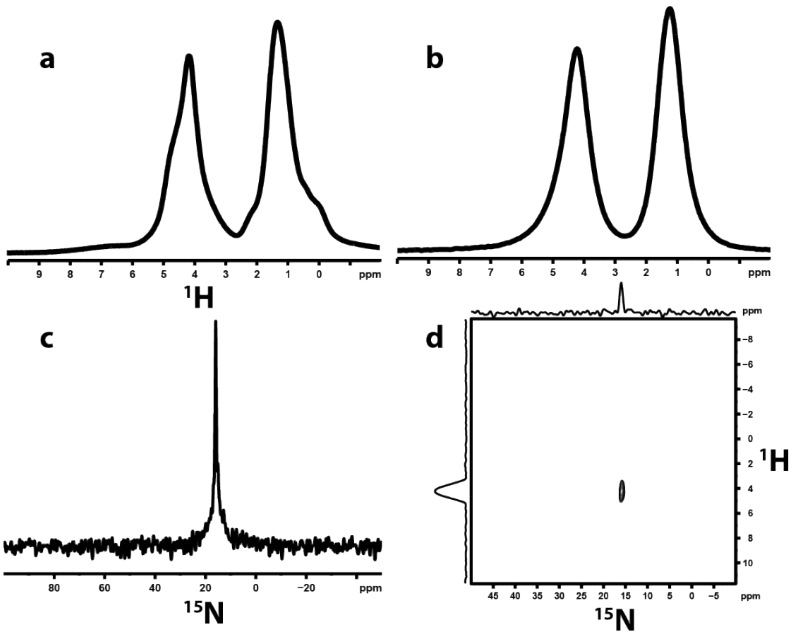

Figure S7: MAS NMR measurements on $^{15}NH_3BH_3$ (700 MHz, ν_R = 60 kHz) for assigning the ^{1}H signals in $Sr(BH_4)_2(NH_3BH_3)_2$. a) ^{1}H, b) DQ filtered ^{1}H, c) ^{15}N, d) ^{1}H-^{15}N.

The full 2D ^{1}H-^{1}H double quantum-single quantum (DQ-SQ) spectrum of $Sr(BH_4)_2(NH_3BH_3)_2$ acquired at 60 kHz MAS using the BaBa pulse sequence is shown in Fig. S8. The spectrum detects spatial proximities between two ^{1}H nuclei in the sample, and the correlations appear at the sum of the chemical shift values of the involved spins in the DQ dimension. It is seen that there are strong correlations between all three types of protons even at the short mixing time of 33.3 μs used. Correlations between hydridic and protic hydrogens are not clearly distinguishable from general H-H correlations, thus the presence of dihydrogen bonds cannot be confirmed, possibly due to highly disordered hydrogen in the structure. However, the correlation between NH_3 and BH_4^- appears stronger than between NH_3 and BH_3 indicating a shorter average distance between NH_3 and BH_4^- compared to NH_3 and BH_3.

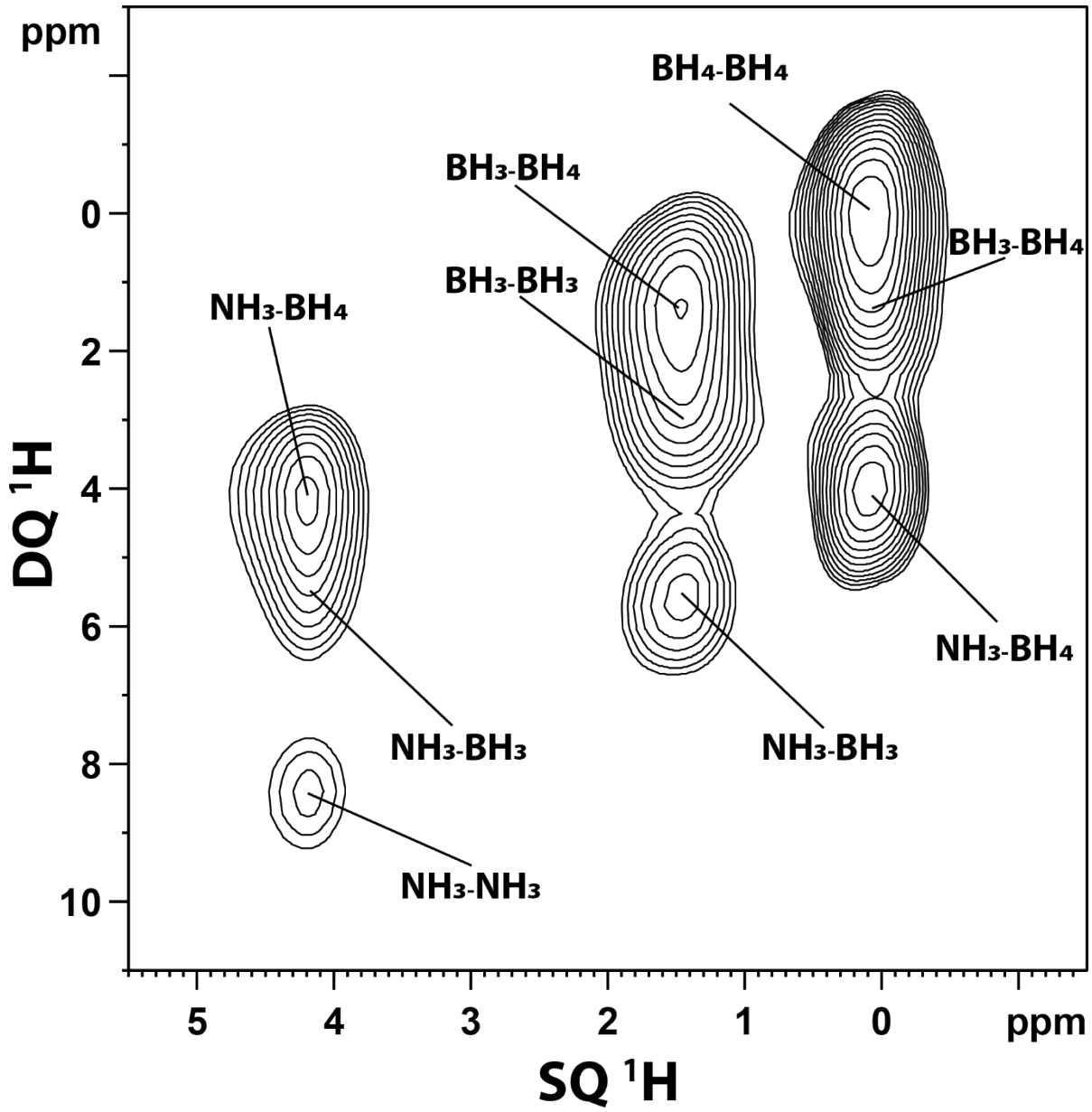

Figure S8: 2D ^{1}H-^{1}H DQ-SQ correlations measured for $Sr(BH_4)_2(NH_3BH_3)_2$ (700 MHz, ν_R = 60 kHz). Correlations between all possible hydrogen pairs are present.

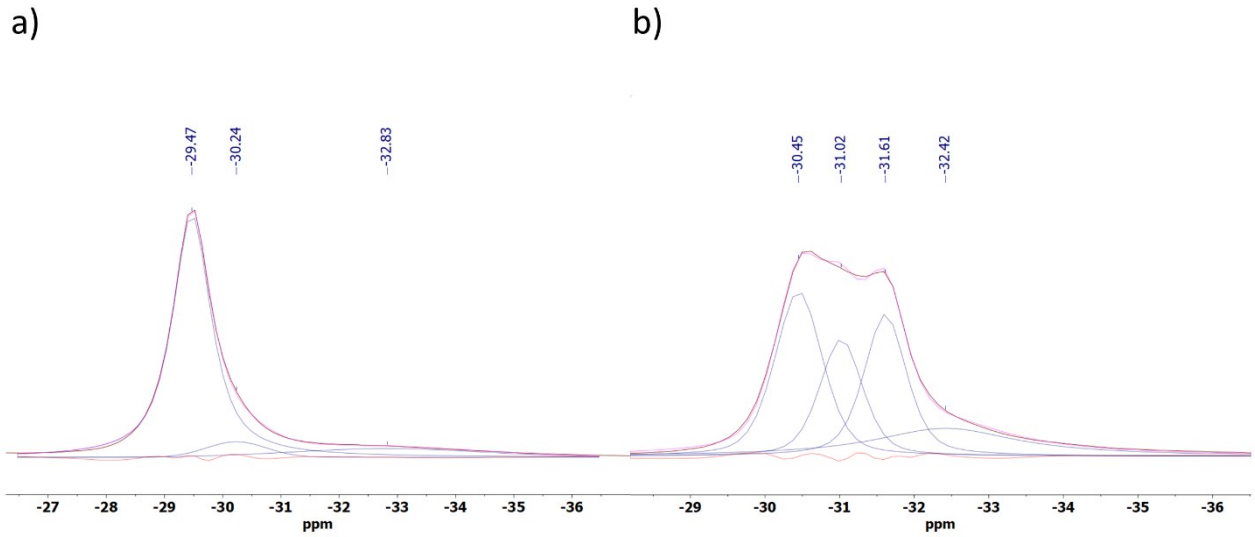

Figure S9: Peak contributions from the different environments of BH_4^- to the ^{11}B MAS NMR spectrum of $Sr(BH_4)_2(NH_3BH_3)_2$ at a) RT and b) 86 °C. The broad peaks at -30.24 and -32.83 ppm in a) and 32.42 ppm in b) are of unknown origin. Table S3 summarizes the parameters.

Table S3: Refinement parameters of the decomposition of peaks in figure S9 for $Sr(BH_4)_2(NH_3BH_3)_2$ at RT and 86 °C.

$Sr(BH_4)_2(NH_3BH_3)_2$ @ RT	Shift (ppm)	Width (Hz)	Area
	-29.47	101	$1.46 \cdot 10^5$
	-30.24	155	$1.04 \cdot 10^4$
	-32.83	500	$1.86 \cdot 10^4$
$Sr(BH_4)_2(NH_3BH_3)_2$ @ 86 °C			
	-30.45	97	$5.42 \cdot 10^4$
	-31.02	87	$3.51 \cdot 10^4$
	-31.61	86	$4.34 \cdot 10^4$
	-32.42	295	$3.51 \cdot 10^4$